2005-07-05

Phase-Matching Optimization of Laser High-Order Harmonics Generated in a Gas Cell

Julia Robin Miller Sutherland
Brigham Young University - Provo

PHASE-MATCHING OPTIMIZATION OF LASER HIGH-ORDER HARMONICS GENERATED IN A GAS CELL

By

Julia Sutherland

A thesis submitted to the faculty of

Brigham Young University

in partial fulfillment of the requirements for the degree of

Master of Science

Department of Physics and Astronomy

Brigham Young University

August 2005

BRIGHAM YOUNG UNIVERSITY

GRADUATE COMMITTEE APPROVAL

of a thesis submitted by

Julia Sutherland

This thesis has been read by each member of the following graduate committee and by majority vote has been found to be satisfactory.

_____	_____
Date	Justin B. Peatross, Chair
_____	_____
Date	David D. Allred
_____	_____
Date	Branton Campbell

BRIGHAM YOUNG UNIVERSITY

As chair of the candidate's graduate committee, I have read the thesis of Julia Sutherland in its final form and have found that (1) its format, citations, and bibliographical style are consistent and acceptable and fulfill university and departmental style requirements; (2) its illustrative materials including figures, tables and charts are in place; and (3) the final manuscript is satisfactory to the graduate committee and is ready for submission to the university library.

_____ _____

Date

Justin B. Peatross
Chair, Graduate Committee

Accepted for the Department

_____

Ross L. Spencer
Graduate Coordinator

Accepted for the College

_____

G. Rex Bryce
Associate Dean, College of Physical and Mathematical Sciences

ABSTRACT

PHASE-MATCHING OPTIMIZATION OF LASER HIGH-ORDER HARMONICS GENERATED IN A GAS CELL

Julia Sutherland

Department of Physics and Astronomy

Master of Science

Ten-millijoule, thirty-five femtosecond, 800 nm (~40 nm bandwidth) laser pulses are used to study high-order harmonic generation in helium- and neon-filled gas cells of various lengths. Harmonic orders in the range of 50 to 100 are investigated. A semi-infinite cell geometry produces brighter harmonics than cells of sub-centimeter length. In the semi-infinite geometry, the gas occupies the region from the focusing lens to a thin exit foil near the laser focus. Counter-propagating light is used to directly probe where the high harmonics are generated within the laser focus and to investigate phase matching. The phase matching under optimized harmonic generation conditions was found to be unexpectedly good with phase zones many millimeters long.

Restricting the laser beam with an 8 mm aperture in front of the focusing lens increases the emission of most harmonic orders observed by as much as an order of magnitude. Optimal harmonic generation pressures were found to be about 55 torr in

neon and 110 torr in helium. The optimal position of the laser focus was found to be a few millimeters inside the exit foil of the gas cell. Probing with counter-propagating light reveals that in the case of neon the harmonics are generated in the last few millimeters before the exit foil. In helium, the harmonics are produced over a longer distance. Direct measurement shows the re-absorption limit for mid-range harmonics in neon has been reached.

ACKNOWLEDGMENTS

I would like to express appreciation to Justin Peatross, my advisor, for his support and assistance. I am also grateful to David Allred and Branton Campbell, members of my committee for their contributions and suggestions.

Mark Adams, Eric Christensen, Nathan Powers, Steve Rhynard, Kelly Smith and Ben Pratt made helpful contributions to the research. I would also like to thank our predecessors in the group who gave us an excellent foundation to build on, and encourage those continuing the research.

I would especially like to express my thanks to my husband, Ammon Sutherland, for his invaluable support.

Table of Contents

List of Figures

Chapter 1:Introduction

1.1 Motivation and Applications for High Harmonics Research

The study of Extreme Ultraviolet (EUV) light is hampered by the fact that the photons are energetic enough to ionize any atom, making the development of optics in this range challenging. Currently, the computer industry is driving growth in this area because small features on computer chips are desirable to improve speed and performance, and the size of these features depends on the wavelength of light used in the lithographic process. Progressively smaller features on chips are necessary to maintain the progress expected in the computer industry, so reliable sources of short wavelength light are in demand [1]. Goals set by computer manufacturers for 2009 require the development of a dependable, high power light source at 13.5 nm as well as the necessary optics. These are among the "key issues that might delay the introduction of the technology" and the fulfillment of the goals of the computer industry [1].

Laser high-order harmonic generation (HHG) is one possible source of EUV light. HHG is not bright enough for the lithographic process itself, but it is a valuable source of coherent, polarized, directional light with wavelengths throughout the EUV that can aid in the development of optical components associated with vital technology. In contrast to the alternative sources of EUV light (such as synchrotron sources), high harmonic generation is modest in size and expense and can be implemented on a table-top scale in a conventional university laboratory.

1.2 Harmonic Generation and Fundamental Concepts

High-order harmonics are generated through the interaction of an intense laser pulse with atoms. The laser intensity needed for HHG in helium is near 10^{15} W/cm^2. In the presence of the strong oscillating electric field of the laser, which can easily be made to exceed 10 V/Å in the focus, electrons are torn from the atoms and accelerated. As the oscillating field reverses direction, it is possible for some of the electrons to return and collide with the parent ion, which releases energetic photons with frequencies that are odd multiples of the laser frequency. Each atom can generate a range of odd harmonics, often many tens or even hundreds of orders, up to a maximum harmonic order that depends on gas species. The wavelength of a harmonic is λ/q, where λ is the wavelength of the laser and q is an odd integer. When the harmonic signals from a collection of atoms in the laser focus constructively interfere, beams of extreme ultraviolet light emerge embedded in the residual laser beam as shown in Fig. 1.1.

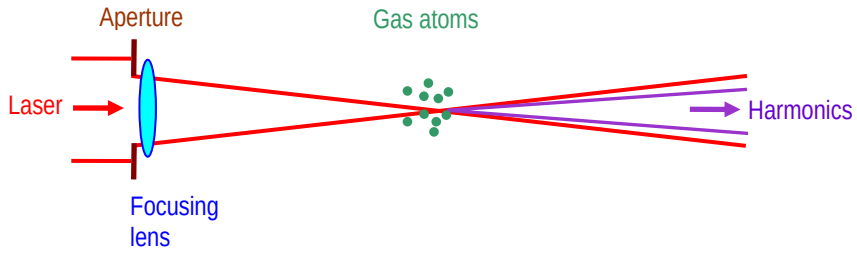

Fig. 1.1 Harmonics generated in a laser focus.

Crystals are appropriate for low-order harmonic generation, but cannot produce high-order harmonics because they are opaque to short wavelengths and would be damaged by the high laser intensities required. Low density gases, on the other hand, are transparent farther into the EUV and are self healing after each laser shot. The maximum

photon energy in HHG increases for atoms with higher ionization thresholds because they endure stronger laser fields before ionizing. Since noble gases have the highest ionization energies, they make good HHG targets [2].

The brightness of each harmonic depends on a complex interplay of several factors. These include phase matching, re-absorption, gas species, and the parameters of the laser. Even when all of these factors are optimized, output for each harmonic order typically has an intensity of only a tiny fraction of the intensity of the generating laser beam. The choice of laser-pulse temporal profile affects the harmonic emission per atom, so one should also consider at what intensity the harmonics are generated and for what duration when assessing conversion efficiency [3-4].

Takahashi et al. produced record conversion efficiencies of 10^{-4} for orders in the teens [5]. Higher orders tend to have markedly lower conversion efficiencies, which limits their use in applications. Nevertheless, high harmonic generation promises to provide a compact (table top), coherent, directional source of light in the EUV range.

A. Phase Matching

In order to generate the largest possible output signal, the harmonic contributions of individual atoms need to constructively interfere. Hence, the harmonics generated upstream in the medium need to be in phase with new harmonics generated downstream, a principle known as phase matching. This implies that the fundamental and the harmonic must have the same phase velocity as they travel through the generating medium so the harmonics stay in phase with the generating pulse. However, there are at least three sources of phase mismatch: geometrical phase mismatch due to wavelength-dependent

diffraction, frequency-dependent index variations, and intensity-dependent variations in the phases of the harmonics as they are emitted from atoms.

Geometrical phase mismatch is due primarily to the Gouy shift, which is a phase change of π that all light beams experience as they go through a focus [6]. The Gouy shift appears as the expression $tan^{-1}\ z/z_0$ in the phase of the electric field of a gaussian laser beam. The Rayleigh range, $z_0=\pi w_0^2/\lambda$, is a parameter that depends on the beam waist, w_0, and the wavelength of the laser [7]. The harmonics are generated with a phase q times that of the laser, where q is the harmonic order. This means that even though the laser has a phase shift of only π as it goes along the focus, the emission of harmonics is associated with a phase that ranges through $q\pi$ through the focus. Thus, a generated harmonic goes in and out of phase many times as the light from different locations combines. The problem is most pronounced for higher harmonic orders. The size of one phase zone (how far a harmonic can travel before it is out of phase by π) at the focus due to Gouy shift varies between 300-700 μm for harmonic orders 50-100 in an f/50 focusing geometry like ours.

Frequency-dependent index is a property of the medium in which the light propagates. This causes the laser and each harmonic to travel different speeds, which means that new harmonics generated by the laser later in the medium will not be in phase with the earlier harmonics generated. Generally, this effect is small in comparison to the geometrical mismatch, but the process of HHG partially ionizes the gas and creates a plasma. In a plasma, the difference in index for the laser versus the harmonics can lead to serious phase mismatches. The index of refraction in a plasma is given by

$$n_{plasma} = \sqrt{1 - \frac{{\omega_p}^2}{\omega^2}} \cong 1 - \frac{{\omega_p}^2}{2\omega^2} \quad \text{, where} \tag{1.1}$$

$${\omega_p}^2 = \frac{Ne^2}{\varepsilon_0 m} \, . \tag{1.2}$$

where N is the number of free electrons per volume and ω is the angular frequency of the light [7]. The plasma frequency is about 2×10^{13} rad/s, assuming a pressure of 100 torr and 5% ionization. For comparison, the laser frequency is 2.2×10^{15} rad/s, two orders of magnitude larger, which yields a plasma index of .999954. The phase difference is about $2\pi q(n_{plasma}-1)L/\lambda$ where L is the distance along the direction of propagation. To find the length of phase zones, we set the phase difference equal π and solve for L. Accordingly, we learn that phase zones near the focus due to plasma index are about 100 μm long. Phase differences due to plasma index have the same sign as phase differences due to the Gouy shift, so the effects compound each other, making overall phase matching worse.

The presence of the plasma in the laser focus can affect HHG and phase matching in other ways, as well. As the laser begins to focus down and ionize the generating medium, the density of free electrons is highest on axis where the beam is most intense and lower in the outer part of the beam. This creates a lensing effect that defocuses the laser, causing significant changes to the laser focusing, phase, and intensity profile. Since the HHG process and the phase of the generated harmonics are strongly dependent on the intensity of the laser beam, this defocusing of the laser can alter geometrical phase matching conditions from what would be expected in the absence of a plasma.

Spatial variations of intensity inherent in the laser beam can also cause phase differences in generated harmonics. The response of individual atoms to the laser field depends on the intensity they experience. In particular, the phase of emitted harmonics

depends on the laser intensity which varies both radially and axially. This is yet another cause of phase mismatches, though it is possible in some situations for these differences in phase to counteract some of the other phase mismatches for an overall improvement.

B. Re-Absorption

Even if phase matching is perfect in a laser focus, the energy of harmonic output is limited by re-absorption in the generating medium. A coherent harmonic signal grows proportional to the squares of the length of the medium and the pressure. On the other hand, as a harmonic beam travels through the generating medium, it is attenuated in proportion to the negative exponential of the same two factors (medium length and pressure).

When both of these effects are combined, it is found that the signal grows for a certain length as the laser interacts with the generating medium, but then any new harmonic generation is offset by the re-absorption of harmonics generated upstream. As the product (pressure × length) gets large, the harmonic signal approaches a maximum value, as illustrated in Fig. 1.2. Thus, as the signal reaches a significant fraction of this maximum it is not worth trying to improve output by increasing the medium length or pressure. In this case, the HHG is said to have reached the "re-absorption limit".

Fig. 1.2 shows a graph of equation 1.3, the harmonic emission as a function of σNL. In equation 1.3, L is the length of a gas generating harmonics, and the quantity $(L-x)$ is how far from the end of the cell a particular harmonic is generated. The parameter σ is the absorption cross section. The fuchsia line shows the half-maximum point, which occurs when $\sigma NL = 2.456$.

$$\mathrm{Sig}(q) \propto \left| \int_0^L N e^{-\sigma_q N (L-x)/2} dx \right|^2 = \frac{4}{\sigma_q^2} \left(1 - e^{-\sigma_q NL/2} \right)^2 \qquad (1.3)$$

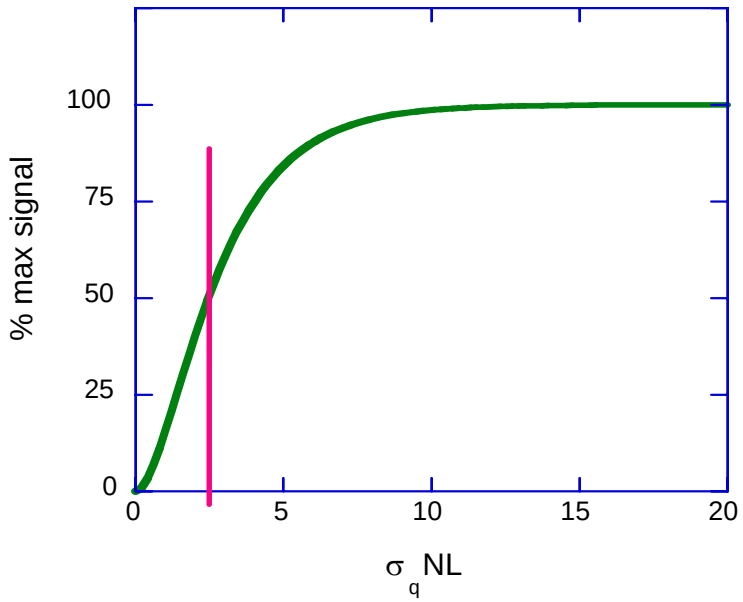

Fig. 1.2 Harmonic signal as a function of the product of length and pressure.

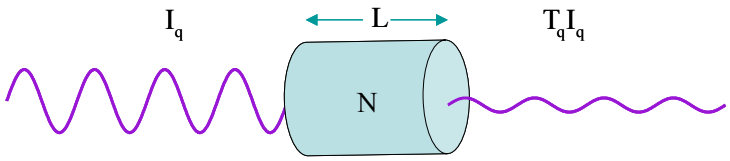

Fig. 1.3 Transmission through a medium of length L containing N atoms/volume.

In the case where a harmonic is traveling through an absorptive medium of length L with no new harmonic generation, the signal is attenuated by a factor of $T_q = e^{-\sigma NL}$. Using our expression for harmonic signal from equation 1.3, we can solve for the equivalent value of T_q that corresponds to the half maximum point where $\sigma NL = 2.5$. We find that the re-absorption limit is reached when T_q drops to 9%, as calculated in equation 1.4.

$$\text{Half Max:}\quad \left(1-e^{-\sigma_q NL/2}\right)^2=\frac{1}{2}\quad\Rightarrow\quad T_q\equiv e^{-\sigma_q NL}=\left(1-\frac{1}{\sqrt{2}}\right)^2=0.09 \qquad (1.4)$$

C. Gas Species

Harmonic emission in gases follows a characteristic spectral pattern with three distinct regions: a steep decrease in magnitude in the first few harmonics, a long plateau where the magnitude gradually decreases, and a sharp cutoff [10].

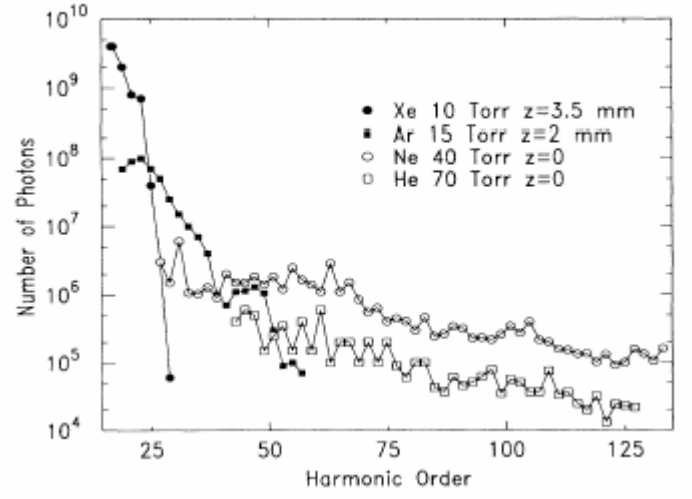

Fig. 1.4 Harmonic emission for xenon, argon, neon and helium as a function of harmonic order. Taken from Ref [10].

Emission is highest for low orders, with the heavier gases producing the brightest signals. Lighter gases can produce higher orders. Helium has the potential to produce the highest order harmonics (theoretically up to $q = 199$ for our 800 nm laser using a semi classical model [2]). The harmonic output for different orders and the dependence of harmonic output on physical parameters such as aperture, pressure and focus position may differ slightly between gas species, though overall trends are generally similar. The highest conversion efficiencies and record energies are reported in argon or xenon, but

only for lower orders, (q less than 20, for example). [11,5] Work on higher order harmonics generally uses helium or neon gas, though recently even higher orders have been reported in doubly-ionized argon [12,13]. These findings are enumerated in section 1.3.

1.3 Current Status of the Field

Several groups have demonstrated high-harmonic generation with coherence lengths sufficiently long to achieve the re-absorption limit. This has been accomplished for high harmonics of moderate order. Rundquist et al. [14] demonstrated extended phase matching in a hollow capillary tube filled with argon, wherein they reported achieving the re-absorption limit for harmonics up to the thirties. They observed conversion efficiencies $>10^{-6}$ (yielding >0.2 nJ per harmonic order generated with 150 μJ laser pulses). An important advantage of this approach is the ability to achieve good conversion efficiency with relatively little laser energy [14]. Tamaki et al. [15] reported similar enhancements in a capillary tube.

Takahashi et al. [16] recently demonstrated a conversion efficiency of 1.5×10^{-5} for the generation of the 27^{th} harmonic in an argon-filled cell. In this case, a 20 mJ pulse with a loose focal geometry produced 0.3 μJ for individual harmonics. More recently they demonstrated 5×10^{-7} conversion efficiency for harmonics up to the 59^{th} order generated in neon, resulting in 25 nJ of individual harmonic energies from 50 mJ laser pulses [17]. Hergott et al. [11] found only slightly lower conversion efficiencies for similar harmonic orders using a gas jet and a loose focusing geometry, wherein they reported reaching the re-absorption limit. Both groups have demonstrated above [5] or

near [11] 10^{-4} conversion efficiencies for harmonic orders in the teens generated in xenon.

Paul et al. [18] demonstrated remarkable enhancement to harmonic orders up to the 71^{st} generated in a helium-filled capillary waveguide with a corrugated inner diameter. They also saw strong enhancement in neon and argon. More recently, Gibson and coworkers [12,13] showed that a corrugated waveguide with a more finely spaced period enabled the production of harmonics well beyond one hundred orders, both from neon and from argon ions. The conversion efficiencies were not reported in their work. Harmonics in this higher range of orders represent an interesting area of research where the potential for significant improvement to phase matching may still be possible, especially in view of the fact that absorption cross sections are lower.

1.4 Previous Work at BYU

Previously in our group at BYU, a high-intensity laser system was designed and built to study HHG. A new strategy for quasi phase matching using counter-propagating light was proposed [19]. Since the coherence length for harmonic generation is expected to be limited to hundreds of microns owing to phase mismatches, it was estimated that there could be several alternating phase zones in the interaction region near the focus where the laser is intense enough to generate harmonics. The assumption was that the signal would suffer from strong destructive interference because of the alternating phase zones.

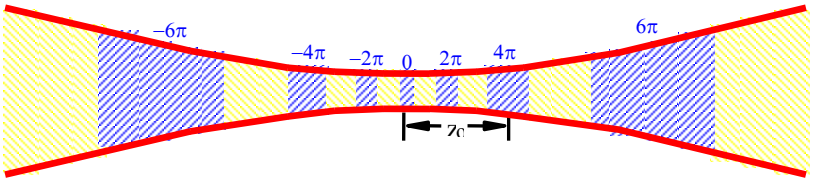

Fig. 1.5 Phase zones near the laser focus due to Gouy shift for $q = 21$.

If harmonic generation could be disrupted in selected out-of-phase zones, the signal from the remaining zones would constructively interfere and result in the enhanced brightness of the harmonics. It was proposed to accomplish this by introducing counter-propagating pulses precisely aligned and interfering with the forward-going harmonic generating pulse in selected zones. The counter-propagating beam is effective at suppressing harmonic generation even when a hundred times less intense than the generating beam. In this case, the counter-propagating beam is weak enough that it does not damage or alter the medium as it passes.

This strategy was modeled by J. Peatross et al. [19], and improvements of two orders of magnitude were suggested to be possible. The experimental apparatus and laser system to implement it was designed by Dr. Peatross and built by S. L. Voronov et al. (For more details see references [20,2].) The setup includes variable delay to control where the pulses collide in the focus and independent chirp control to adjust the temporal profile of each beam. S. Voronov et al. demonstrated the validity of this scheme. They demonstrated an enhancement of the intensity of the 23rd harmonic in argon by two orders of magnitude in a case of poor phase matching [2].

1.5 Outline of Experiments

This thesis represents a continuation and extension of the earlier work with counter-propagating light. Since I joined the group, we have focused on harmonics of orders 50-100 generated in cells filled with neon or helium. The capacity to suppress harmonic generation in a particular region makes the counter-propagating beam useful as a probe to show where in the laser focus a particular harmonic beam originates.

We have documented how manipulating various parameters changes the harmonics generated [21]. First, we demonstrated how aperturing the beam before focusing can enhance harmonic production. Next, we investigated how harmonics are affected by the position of the laser focus with respect to the exit foil of the cell. Then, we studied how pressure in the cell influences the harmonic signal. Additionally, we systematically compared short cells (1-6 mm in length) to a "semi-infinite cell", where the generating gas fills the region from the focusing lens to a single exit foil. The effect of re-absorption was also studied by introducing a second cell later in the laser path after the beam was too weak to generate additional harmonics. These experiments were performed for the most part with the existing hardware and laser system. With the system parameters optimized, we used counter-propagating light to probe the extent of phase matching in the laser focus.

In addition to performing and analyzing experiments, a significant contribution I made to the experimental configuration was the integration of a new data capture system. This involved extensive alteration and debugging of existing Labview code and the writing of additional software that interacts with another computer via GPIB. The new system controls the capture, storage and processing of the data. Additionally, I obtained

the data presented in this thesis with the aid of undergraduate students that I helped to train and supervise.

The publishing of our data in movie format was especially appropriate in our case, and conveyed subtleties of the effects of parameter manipulation that were not as readily apparent in the graphs of the data, or even presentations of several frames on a page. Some of these movies are available in Ref. [22], which can be found online.

1.6 Outline of Experimental Findings

Our study of the effects cell size, counter-propagating light, aperture size, focal position, re-absorption and pressure on harmonic signal has allowed us to characterize the dependence of harmonic intensity on these parameters and better understand the mechanisms of HHG.

A strong enhancement to the harmonic signal occurs when the laser beam is partially restricted with an aperture before the focusing lens. The aperture effect that we observe is similar to that reported by Kazamias et al. for lower-order harmonics generated in an argon-filled cell of finite length [22].

Changes in the shape of the harmonics observed (angular distribution) and different behavior between moderate order harmonics and the highest order harmonics were observed during many of the scans. This suggests that changing the aperture may be effecting directional (off-axis) phase matching. Analyses done to explain the aperture effect generally ignore off-axis effects. Interesting variations of phase and intensity appear when these effects are considered. Behavior that differs between different orders of harmonics implies that optimal phase matching conditions are different for different

frequencies, but can be adjusted to favor the preferred orders of harmonics. Mechanisms such as self focusing of the laser may help explain these results, which will be investigated by other members of our group in the future.

We characterized the dependence of harmonic emission on focal position and pressure. The optimal pressure we found for HHG was 55 torr in neon and 110 torr in helium. The optimal focal position was found to be a few millimeters upstream from the exit foil. These results are described in detail in Chapter 3.

Brighter harmonics are produced in a semi-infinite cell than in short cells of 6 mm or less. This, as well as the comparative simplicity of the setup, has made the semi-infinite cell our preferred cell option for HHG.

Our probing of harmonic emission with counter-propagating pulses shows that harmonics are phase matched over a much greater distance than expected, so much so that in most cases, only a single phase zone near the exit foil was found. The harmonics were well enough phase matched that the re-absorption limit was reached in the case of neon. This was quite unexpected, since phase mismatch from any one of the possible sources (e.g. geometrical), should be severe enough to create many opposing phase zones within the HHG region.

The conclusion is that our optimization of the various parameters to produce visibly bright harmonics creates a phase-matched situation. Thus, when the counter-propagating light was used to suppress harmonics in regions near the focus, no out-of-phase zones were found or else an enhancement would have occurred. Phase zones were probed and documented under less ideal harmonic generation, and in this case it was possible to enhance harmonic production with quasi phase matching, but the

enhancements did not result in better harmonics than the optimized case with no counter-propagating light.

1.7 Overview

Section 2.1 describes the laser system, including the parameters and the delivery of the laser beam, for both the forward-going and counter-propagating pulses. The section covers control and characterization of the temporal profile of the counter-propagating pulses as well as the delivery of the beam to the experiment.

Section 2.2 describes the layout of the experiment itself, including the positioning of the short or semi-infinite cells within a series of vacuum chambers for differential pumping. It also describes the beam path the laser and harmonics travel and explains the procedures for detection, imaging and data capture. Section 2.3 details the function of the data acquisition software and the general procedures for scanning.

Section 2.4 describes the manipulation of the parameters we used to characterize harmonic generation such as focal position, aperture diameter and pressure. Section 2.5 explains our method of controlling the counter-propagating beam and details our comparison of different cell lengths and measurement of re-absorption.

Chapter 3 presents data showing how harmonic generation varies as the parameters outlined in Chapter 2 change. Chapter 4 outlines our conclusions resulting from the data presented, expanding on the findings summarized in section 1.6.

Chapter 2: Experimental Apparatus and Procedure

2.1 Laser System

The laser used for the present experiments delivers about 10 mJ per shot at a repetition rate of 10 Hz. The 800 nm pulses (~40 nm bandwidth) are compressed to about 35 fs, measured by auto-correlation. The laser intensity needed for harmonic generation in helium is about 10^{15} W/cm^2. Our energy and pulse length along with a focal radius of 75μm correspond to a peak intensity of ~10^{16} W/cm^2 at the focus. For more details on the laser system, see the doctoral dissertation of S. Voronov [2]. The counter propagating beams are split from the main beam before final amplification and compression occurs. They are compressed independently from the forward beam. Up to five counter-propagating pulses with adjustable duration (down to 35 fs) and spacing can be provided to the experiment. Finer temporal structure for the counter-propagating beam can be obtained by overlapping two of the individual pulses and causing them to beat. A longer pulse can be formed by combining more than one of the five available pulses. When all five pulses are lengthened and spaced so they just overlap, a ~10 ps pulse can be generated that interacts with the forward beam over a distance of ~2 mm.

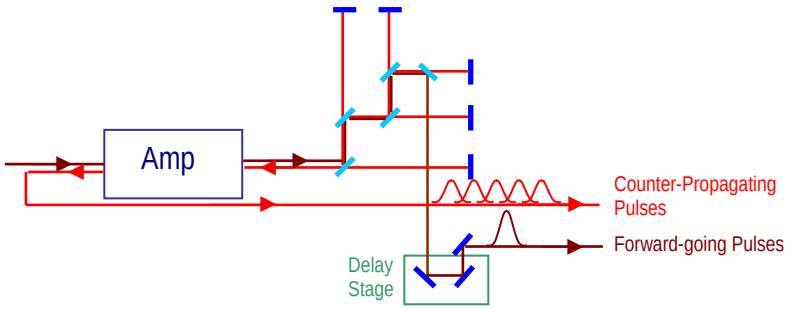

Fig. 2.1 Schematic of the pulse production and amplification portion of the laser system.

Fig. 2.1 shows the portion of the laser system where the counter-propagating pulses are produced and amplified. The five beam splitters that separate the counter-propagating pulses from the main pulse are shown in light blue. The forward-going beam subsequently travels on a separate delay path that includes a variable delay stage to synchronize it with the counter-propagating pulses for the experiment. The adjustable stage makes it possible to control the location within the chamber where the forward and counter-propagating pulses collide. After the beam splitters, the counter-propagating beam undergoes final amplification. Once the beams leave the amplification area, the forward and counter-propagating pulses are compressed using separate diffraction gratings and travel towards the experiment. Just after compression, samples of each beam are split from the main pulses and redirected for auto- or cross- correlation.

Auto-correlation can be used to measure the temporal profile of the main pulse, while the temporal profile of the counter-propagating beam and the spacing of the individual counter-propagating pulses can be measured using cross-correlation with the main pulse. For auto-correlation, a sample of the main pulse is split into two pieces and the pulses mix in a nonlinear crystal. Cross-correlation is similar, but in that case the counter-propagating beam mixes with the main pulse. The doctoral dissertation of S. Voronov explains the details of the correlation measurement apparatus [2].

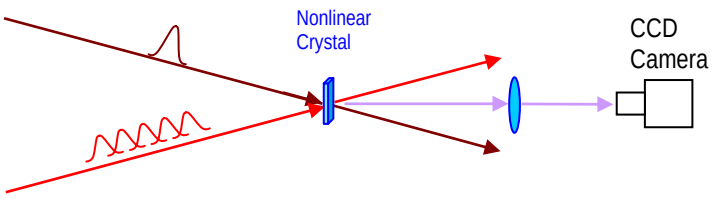

Fig. 2.2 Schematic of cross correlation.

As depicted in Fig. 2.2, the interaction of the two beams in the nonlinear crystal maps the temporal profile of the pulses into a spatial distribution of light which is focused by a lens and imaged by a CCD camera. An image of cross-correlation measurement involving five short counter propagating pulses is shown in Fig. 2.3.

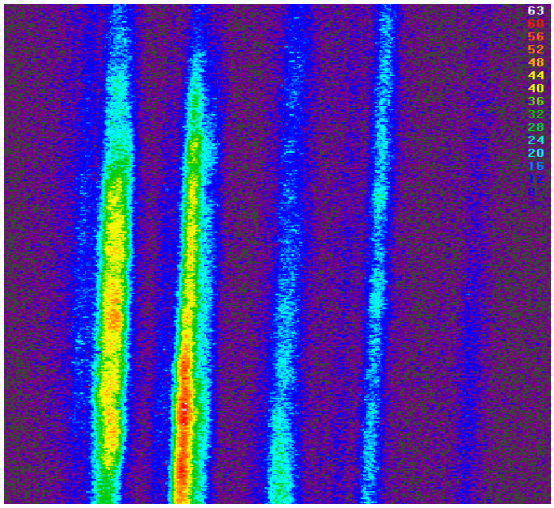

Fig. 2.3 Cross correlation image of the five counter-propagating pulses.

2.2 Experimental Setup

The main laser pulse is focused using f/50 optics into a gas cell where the harmonics are generated. The end of the cell is capped with a molybdenum foil. Prior to the experiment, the laser is used to drill a hole in the foil to allow the harmonics to exit the cell. We have also made short cells a few millimeters long where both ends are

capped with a molybdenum foil. In this case, the cell is positioned near the focus and the laser drills both entrance and exit holes.

As seen in Fig. 2.4, the main laser pulse enters the vacuum chamber from the left. The counter-propagating light enters the chamber from the opposite direction, reflecting off a mirror with a 2.5 mm hole. This hole provides an avenue for the harmonics to reach the detector while directing about half of the energy in the counter-propagating beam towards the area where the harmonics are generated. The profile of the counter-propagating beam is ring shaped just after the mirror. However, the energy moves into the axis as it focuses, and the spot at focus is similar in width to the focal spot of the forward going beam. [20]

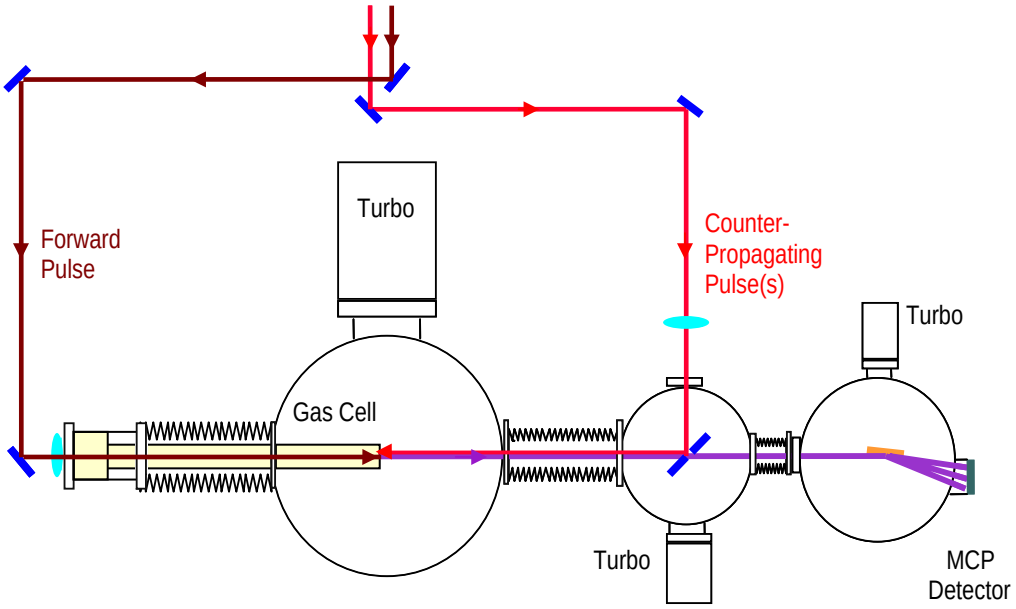

Fig. 2.4 Layout of experiment. The laser main generating beam and the counter-propagating beam enter from opposite directions and collide near the exit of the gas cell.

Fig 2.4 shows the paths of the forward and the counter-propagating beams as they enter the experiment. The purple beam represents the harmonics as they exit the gas cell into the vacuum and travel towards the detector. Three vacuum chambers are separated

by small holes that allow the light to pass, but make differential pumping possible. This allows the pressure in the last chamber to be held at ~10^{-6} torr, which is necessary for the proper function of the detector. The harmonics are deflected from a diffraction grating (1200 lines/mm, 2 m radius of curvature) that separates each harmonic order according to wavelength. The curved grating substrate focuses each harmonic to a vertical line on a microchannel plate (MCP), so that the angular divergence of the harmonic in the vertical dimension preserved. The MCP is coupled to a 30 mm diameter phosphor screen on which the harmonic orders appear as vertical stripes.

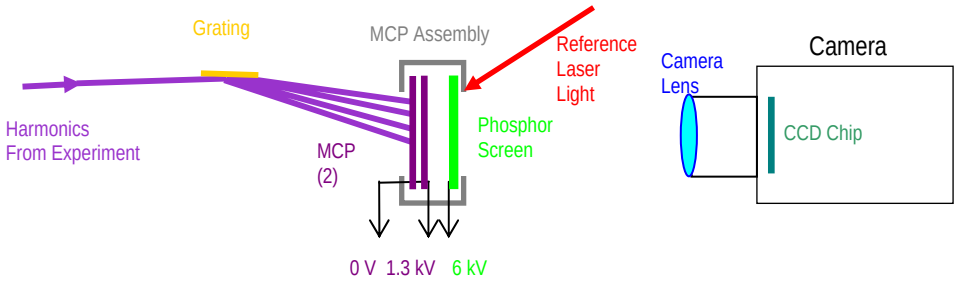

Fig. 2.5 Top view of harmonic detection system.

Fig. 2.5 illustrates how the harmonics are detected. Harmonic photons striking the first MCP excite a localized shower of electrons that cascade through a voltage difference of 1300 V inside the tiny spatially separated channels of the plates. After being accelerated across an additional voltage of 4700 V, the electrons impact the phosphor screen, creating a glowing image of the harmonics. The image is recorded by the CCD camera and captured by the computer.

To provide a comparison of laser energy, an attenuated beam of light from the main laser beam is focused on the outside of the phosphor screen next to the harmonic image. This tiny laser spot becomes part of the image, so each frame of harmonics records a measure of the laser power for that shot. It then becomes possible to reduce

variations in the data due to fluctuations in laser power by saving only those frames with acceptable laser power and discarding data from laser shots with energy that fluctuated out of range.

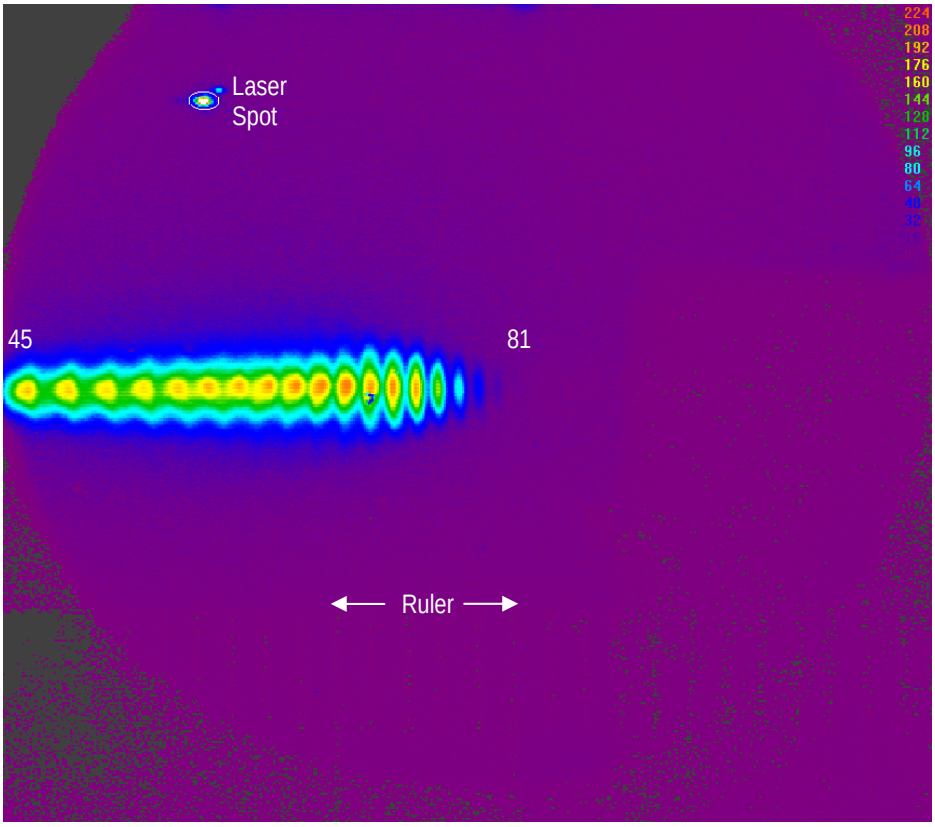

Fig. 2.6 Harmonic orders 45-81 on the phosphor screen. The laser spot is used for laser power comparisons. The ruler is used for calibration to determine which harmonic orders are visible.

Fig. 2.6 shows the appearance of the harmonics as imaged at the computer. Each odd harmonic appears as a separate stripe, with color representing intensity according to the legend. The laser spot is used to filter the data according to laser power. The round outlines on the left are the edges of the phosphor screen, and the millimeter ruler faintly visible across the lower part of the image is used for calibration to determine which harmonic orders are in view. This image shows harmonic orders 45-81. The calibration scheme is described in detail in the honors thesis of Kelly Smith [24].

2.3 Data Acquisition and Scanning

Since our laser power can fluctuate greatly from shot to shot, a computer program allows the user to select an acceptable range of laser power before a scan begins. The program samples the laser energy for about 100 shots and plots a histogram of the results. A graphical slide bar along the x axis of the histogram allows the user to select minimum and maximum acceptable values for laser power. A range of ±10% from the mean laser energy per shot was generally adequate to produce good quality data unless the laser had unusually large drift. The frames where the laser power is outside this range are discarded as the data is taken. The program continues to take data until the requested (usually 20) number of frames with acceptable laser power is reached. An error is generated if this takes longer than several seconds (i.e., the majority of shots are being rejected). This keeps the data and results from being distorted by drift in laser power, and also reduces noise, since fluctuations in laser power can be a significant source of irregularity and ambiguity in the data. After the scan is over, the saved frames for each data point are averaged together, background intensity is subtracted, and data is extracted in one of three possible formats. The brightness of selected harmonics can be collected and graphed. Bitmap images of the frames can also be exported for use as pictures or movies. In addition, a "line out" of intensity across all harmonics can be plotted.

2.4 Variable Parameters

We investigated several parameters in order to better understand the HHG process and optimize harmonic output. This section describes our procedures for studying cell length, aperture size, focal position and the pressure of the generating gas. In general, each parameter was scanned over a range, and 10 or 20 frames for each data point were saved. The frames to be saved can be selected by laser power as described in section 2.3, or all of the frames up to the specified number can be saved without regard to the laser power.

To compare short cells with the semi-infinite cell, each cell was installed in turn, with the other parameters optimized. The best harmonics from each were compared to determine which cell was preferred.

Aperture scans are performed by using a set of calipers to adjust the aperture width to a specific diameter for each data point. Aperture size was varied in half-millimeter or millimeter increments.

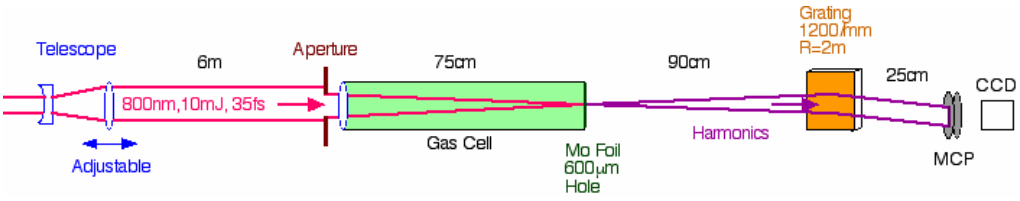

Fig. 2.7 Schematic of experimental layout with original focus position adjustment. In the altered layout, the first converging lens is made stationary and the second is made adjustable, with a window added as the entrance to the cell.

Scans of focal position with respect to the exit foil (or "z scans") were performed by changing the position of a lens on a stage early in the laser system to adjust the position of the focus relative to the exit foil of the gas cell. The lens was moved in millimeter increments. Though this yielded useful data, we did observe one disadvantage: the movement of the lens subtly changed the collimation of the beam as it traveled

through the compression gratings, which were designed to work on a collimated beam. Since the effects of this change were difficult to account for, we later modified the system to adjust the focusing lens itself so that the beam at the gratings remained collimated. To accomplish this, a window was added as the entrance to the gas cell, and the focusing lens was mounted on a movable stage immediately before.

Pressure scans were performed by adjusting the pressure of the gas in the cell in 5-torr increments. These scans had to be completed quickly, because at the highest gas pressures (for helium) the vacuum pumps would become overloaded. Since this problem only occurred at the highest pressures, it was possible to manage it by turning down the pressure between data points.

2.5 Counter-Propagating Light and Absorption Measurements

In using the counter-propagating beam as a probe, we found that a single short counter-propagating pulse was insufficient to suppress harmonic generation over a long enough region. Several pulses were combined to form a longer pulse. Most counter-propagating experiments were performed with all five counter-propagating beams, each chirped out to ~2 ps and spaced to approximate a single pulse ~10 ps long, so as to destructively interfere with the forward going beam over a region ~2 mm long.

Scans using the counter-propagating beam were performed using a computer program that controls a motor on the beam delay translation stage as well as data capture. Each scan produced a selected number of data points (usually around 100), and a motor moved the delay stage incrementally through a selected distance (typically 6-10 mm full range). The incremental movement of the delay stage causes the point at which the

counter-propagating pulse collides with the main pulse to move by the same amount. During the course of the scan, the crossing point of the two beams encounters the region where the harmonics are being generated, which causes harmonic emission to be suppressed. After the scan is over, the saved frames are processed, and numerical data is extracted and graphed.

Absorption was studied independently from harmonic production to confirm the effect that traveling through the gas has on previously generated harmonics. A second cell was placed in the beam path far enough from the focus that there was no chance of additional harmonic generation, as shown in Fig 2.8. The cell was 78 mm long and the pressure of neon in the cell was varied in ~0.3 torr increments. A similar scan was made in helium, with the pressure varied in 1 torr increments.

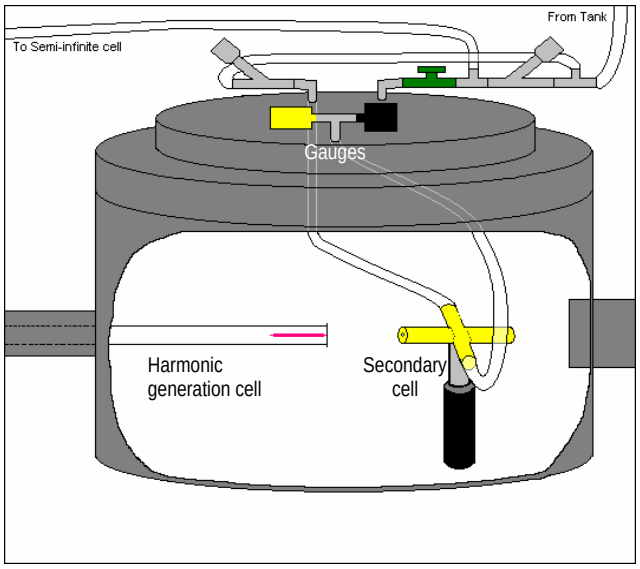

Fig. 2.8 Vacuum chamber configuration for direct absorption measurements. Different gauges were used for measurements in helium and neon.

Chapter 3: Experiments

3.1 Short Cells vs Semi Infinite

Fig. 3.1 shows an image of high harmonics generated in helium as seen on the MCP. As mentioned in section 2.2, the angular divergence of the harmonics is preserved in the vertical dimension. The full height of the image is about 6 mrad, indicating that the harmonic beams are restricted to 1-2-mrad divergence angle. The generating laser beam was focused at the exit foil (under vacuum conditions). Self-focusing of the pulse pulled the focus inward, perhaps by centimeters. The pressure for this measurement was set at approximately 130 torr and the aperture before the focusing lens was restricted to ~8 mm, which gave the strongest output signal for most of the harmonics seen.

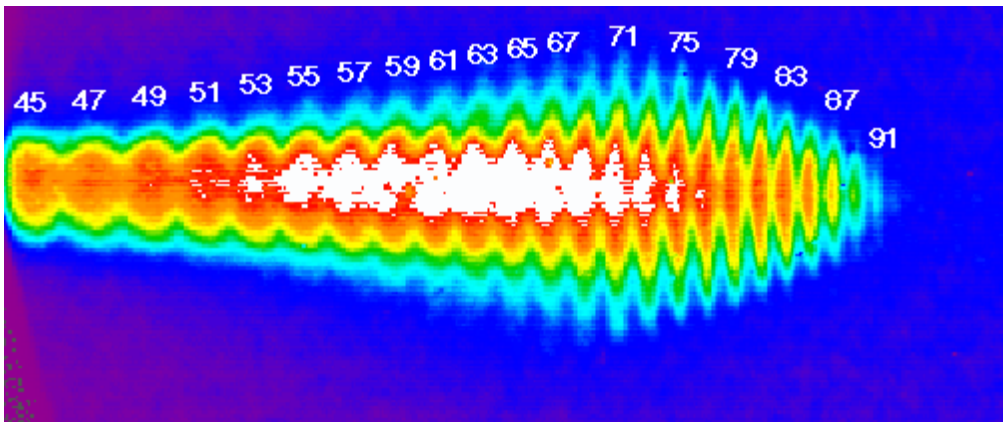

Fig. 3.1 Harmonics generated in helium at 130 torr in a semi-infinite cell**.**

The harmonics seen in Fig 3.1 were acquired using the semi-infinite cell geometry. For comparison, Fig. 3.2 (a)-(c) show the harmonic signal obtained from 1 mm-, 2 mm-, and 6 mm-long gas cells, respectively, filled with helium at approximately 130 torr. In each case, the cell was positioned at a location near the focus, which produced the strongest possible signal. For all three measurements, the aperture

near the lens was set to ~8 mm, which gave optimal output; the signal was an order of magnitude weaker with the aperture open. As is evident, the signal from the semi-infinite cell is significantly stronger. The same trend was also observed in neon-filled cells, although less pronounced. An increase in cell length generally produced a higher signal, but it increased by only about a factor of two from the 1 mm cell to the semi-infinite cell. Because the semi-infinite cell produces the strongest signals, we have worked mainly with that configuration.

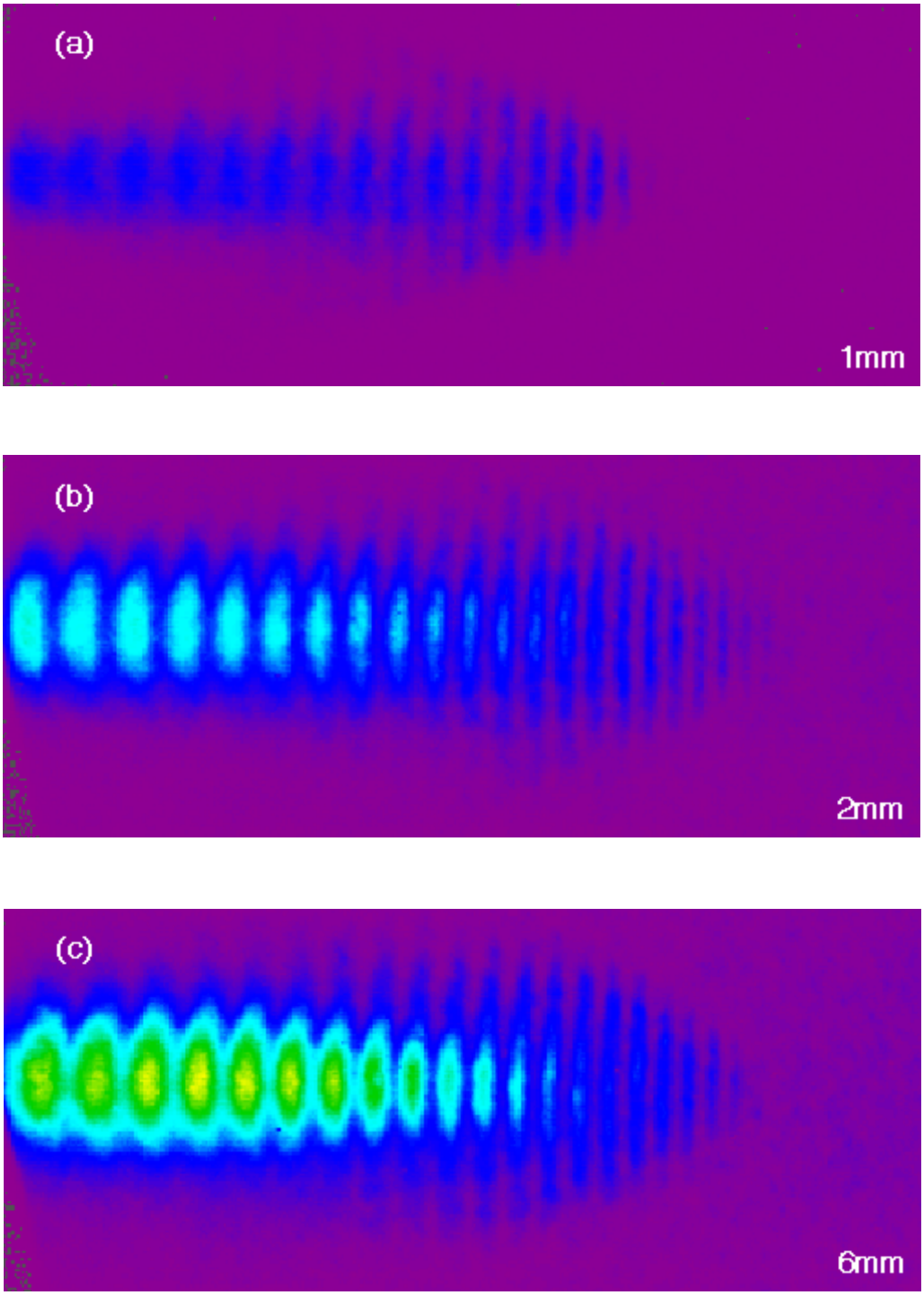

Fig. 3.2 Harmonics generated in helium at 130 torr in (a) a 1mm cell, (b) at 2 mm cell and (c) a 6mm cell.

3.2 Aperture Diameter

As mentioned in Section 1.6, Kazamias et al. reported marked enhancements to harmonic generation in an argon-filled cell when a partially closed aperture is placed in the path of the laser beam before the focusing lens [23]. They observed enhancements of four to ten times for harmonic orders in the twenties. We have observed a similar aperture effect in both finite and semi-infinite cells, in our case for higher orders, generated in neon and in helium.

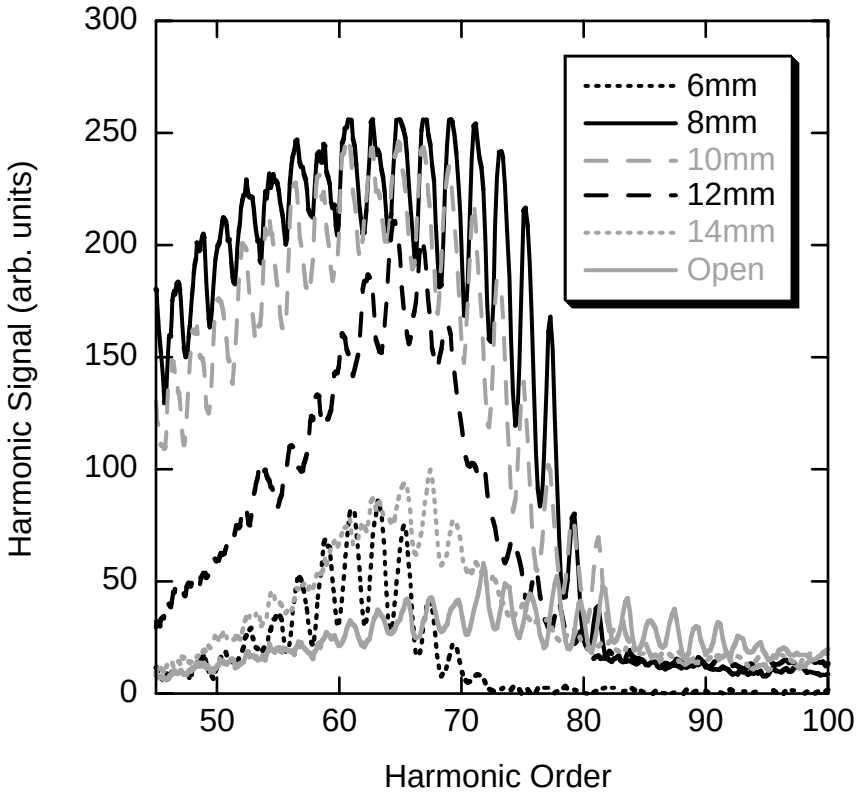

Fig. 3.3 Cross section of harmonic intensity in helium in a semi-infinite cell for several beam aperture diameters.

Fig. 3.3 shows a "line out" of harmonic intensities for harmonics generated in 110 torr of helium for a few different laser apertures. Most of the harmonic orders increase strongly when the beam is significantly restricted by the aperture. The most pronounced results occur for an aperture diameter near 8 mm, compared to the original

beam diameter of about 12 mm. Mid-range harmonics (near 70) increase in brightness by a factor of 15, but higher orders increase less, if at all.

Fig. 3.4 shows a scan of harmonics as a function of aperture diameter taken with neon. The behavior is similar to that of helium. Harmonics in the 50s and 60s improve by over an order of magnitude, but the highest order harmonics improve less, in this case the harmonics in the 70s improve by a factor of eight. Fig. 3.5 shows images of the harmonics in both helium and neon for a range of aperture diameters.

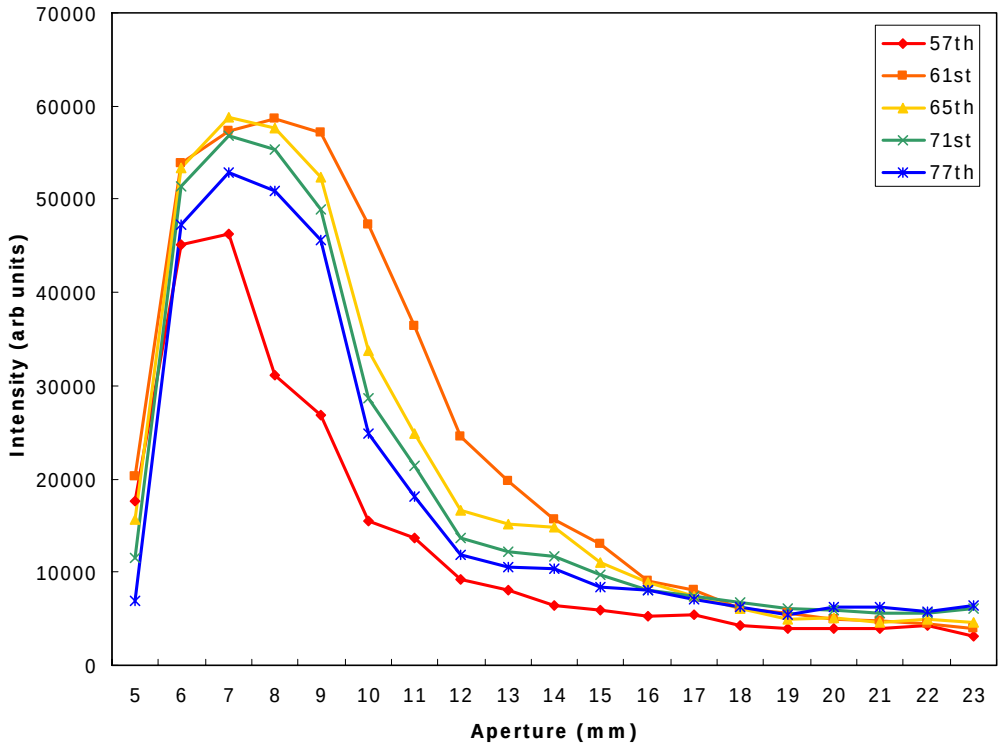

Fig. 3.4 Intensity of selected harmonics in neon as a function of aperture.

Kazamias et al. identified the effective f-number, the laser-beam spatial quality, and the interplay between the laser phase and the intrinsic phase of high harmonic emission as the primary causes for enhancements to high harmonic intensity as the aperture closes [23]. We investigated whether the aperture effect could be explained

primarily by a change in the effective f-number of the beam by installing a longer focal-length lens (and extending the tube on the vacuum chamber). This increased the f-number by 67%, but it could not reproduce the bright harmonic signal observed with the shorter-focal-length lens and the restricted aperture. Apparently, the aperture introduces phase variations on the laser wave front that are favorable to phase matching.

Although we cannot eliminate the possibility that the increase in harmonic signal as the aperture closes is due to improved spatial quality of our beam (i.e. throwing away distorted portions of the beam), we believe that the enhancement would occur even if our beam were a diffraction-limited Gaussian. Our laser focuses to within 20% of the diffraction limit. Also, we observed similar behavior when restricting the aperture even when our laser beam quality was degraded by damage to optical components.

In the semi-infinite cell, the pulse likely undergoes nonlinear effects such as self-focusing as well as wave-front distortions from ionizing electrons. These have the potential for influencing phase matching, especially over an extended propagation distance as in the semi-infinite cell configuration. Nevertheless, we have observed the aperture effect in a 1mm-long gas cell, also, which suggests that conditioning of the beam via propagation within the medium is not critical to the effect.

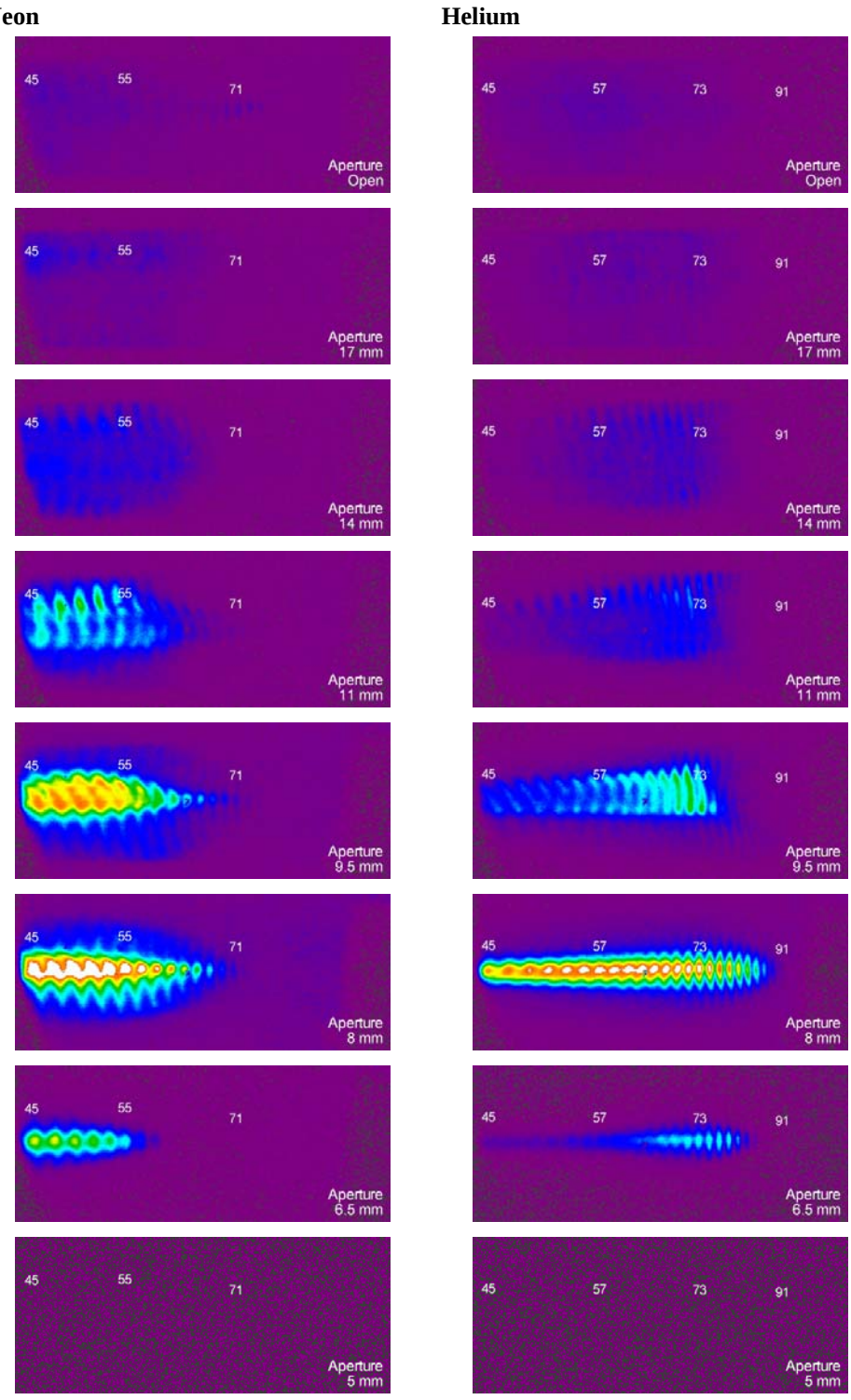

Fig. 3.5 Harmonics in neon and helium for several different aperture diameters.

3.3 Focal Position

When the cell is filled with gas, a gas-species and pressure dependent self-focusing of the pulse pulls the focus inward from the foil by several centimeters. The harmonic production depends on the position of the laser focus relative to the exit foil. We scanned the focal position to find the optimal location. Harmonic signal for a range of focal positions is shown in Fig 3.6 for neon and helium. The pressures were held at 55 torr and 115 torr, respectively. The lower portion of each frame is a digital photo of the gas cell taken from the side that shows recombination light from a streak of plasma produced as the laser focuses in the gas, which allows us to see the relationship between the focus and the exit foil. The scale marker is aligned with the foil to mark the position of the end of the cell. The focal position indicated for each frame represents the focus position under vacuum conditions, with negative numbers inside the cell and positive numbers outside the cell. The actual position of the laser focus may be modified by nonlinear interaction with the gas. The aperture was set at 8 mm for these scans.

The similarities between the two gases are evident. Although helium produces significantly higher orders, the evolution of the spatial structure of the emerging beams as a function of focal position looks very much like that for neon. The angular divergence of the harmonics (i. e., the height of the stripes), which is fairly narrow, varies with focal position and with harmonic order. For some focal positions, harmonic emission is directed narrowly along the axis within a 1-mrad beam. At other focal positions, emission of some of the higher harmonics forms a 3-mrad ring structure.

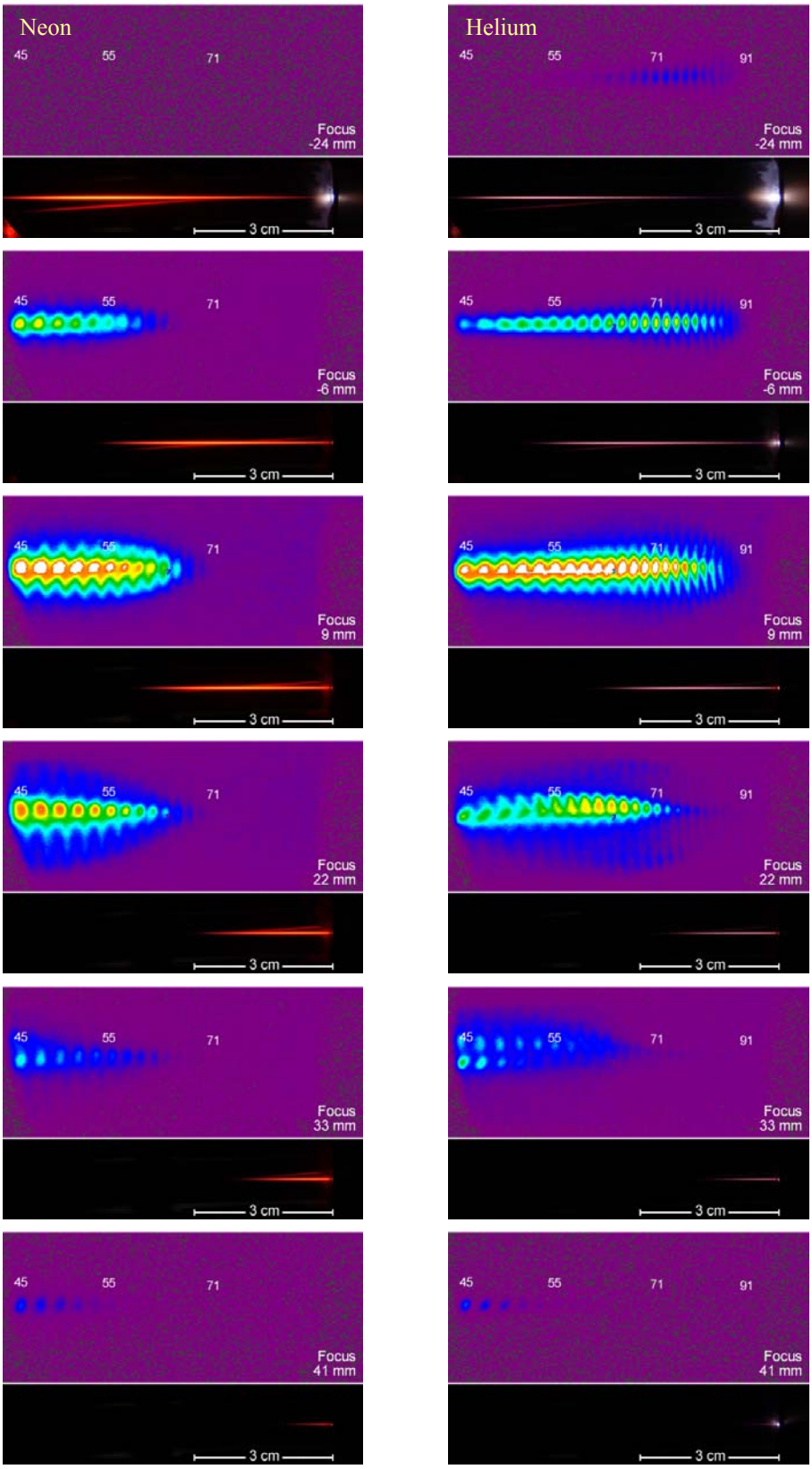

Fig. 3.6 Harmonic signal and image of focus for several focal positions.

3.4 Pressure

Figs. 3.7 and 3.8 show selected frames from scans varying pressure in neon and helium. The most evident general trend revealed is that the harmonic signal improves as pressure is increased up to an optimal pressure, after which further increases in pressure cause a drop in brightness. These scans were performed with optimal aperture setting (8mm) and optimal focal position near the exit of the cell. The optimal pressure was around 55 torr for neon and around 110 torr for helium. The optimal pressures can vary with differing aperture and focal settings, but only gradually.

Though the different harmonic orders achieve maximum brightness very close to the same pressure in a particular gas, there are differences in their response to pressure. In helium, the lowest orders (in the 50s and 60s) start being visible from pressures as low as 20 torr and build slowly until the optimal pressure of 110 torr, after which they drop off rapidly. The higher order harmonics (in the 70s and 80s) require higher pressure to become visible, but they attenuate more slowly than the low orders after the optimal pressure. At the highest pressures, only the highest order harmonics are visible at all. Neon does not generate harmonics above the low 70s, so this trend is not visible in the neon scan.

Another trend of harmonic behavior is the changing shape of the harmonics as pressure is varied. In both neon and helium, the harmonic lines are taller (have a greater angular divergence) for low pressures, and concentrate into a narrower band as pressure is increased. At low pressures, the energy for some harmonics is unevenly distributed; instead of most of the intensity being in the center of the stripe, there are significant concentrations on the edges, sometimes with very little energy in the center at all. This is

evident in helium at 65 torr (see Fig 3.8). Occasionally, the harmonic intensity is concentrated in both the center and edges of the stripe, with less energy in regions in between, as in neon at 20 torr (see Fig 3.7), which suggests that pressure may influence off-axis directional phase matching. Features of pressure scans resemble patterns visible in the focal-position scans of the previous section. Though the scans are not completely analogous, the similarities are logical; increasing pressure likely causes the laser focus to shift position due to increased interaction with atoms of the generating medium.

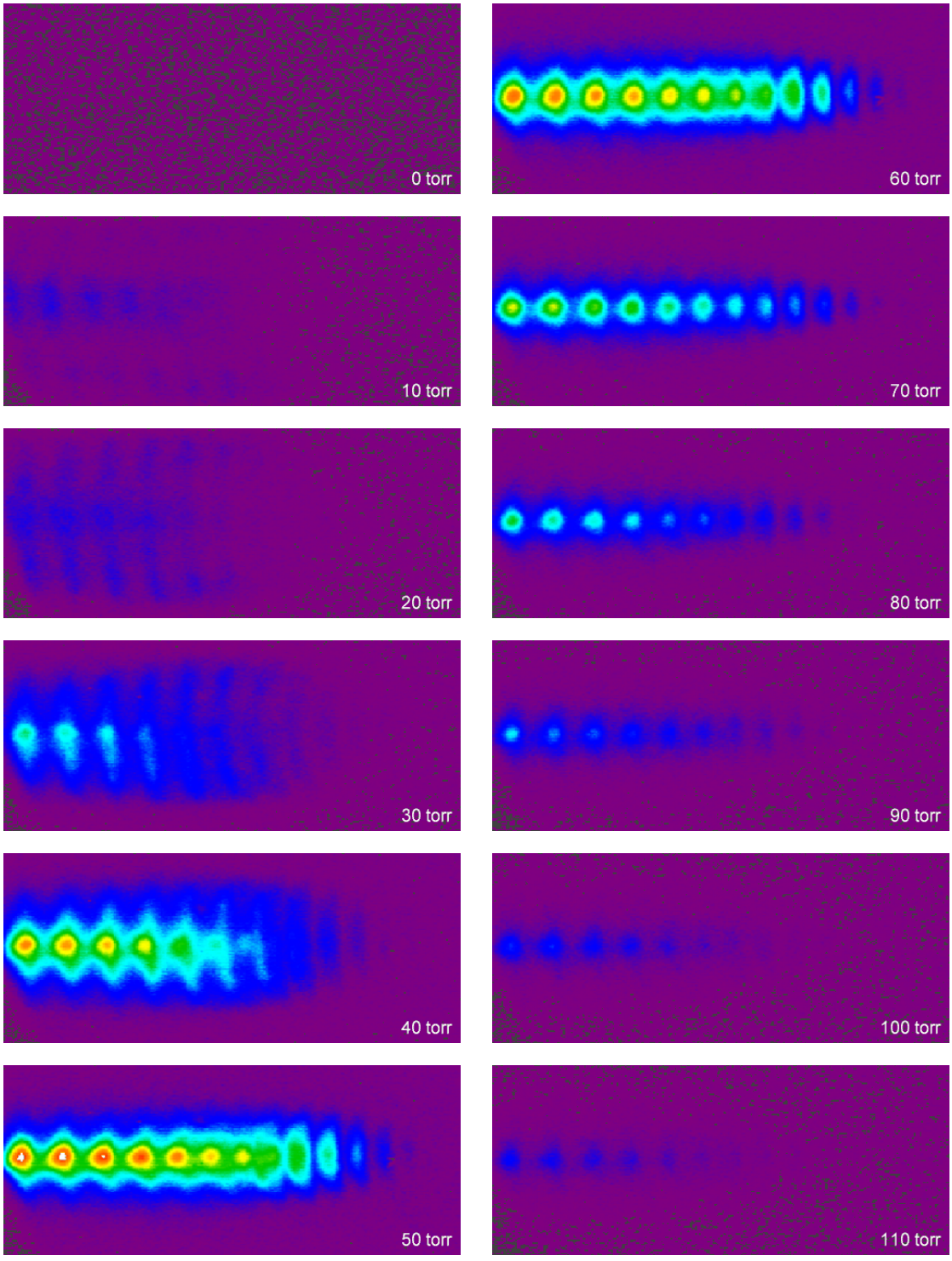

Fig. 3.7 Harmonic signal for several different pressures in neon.

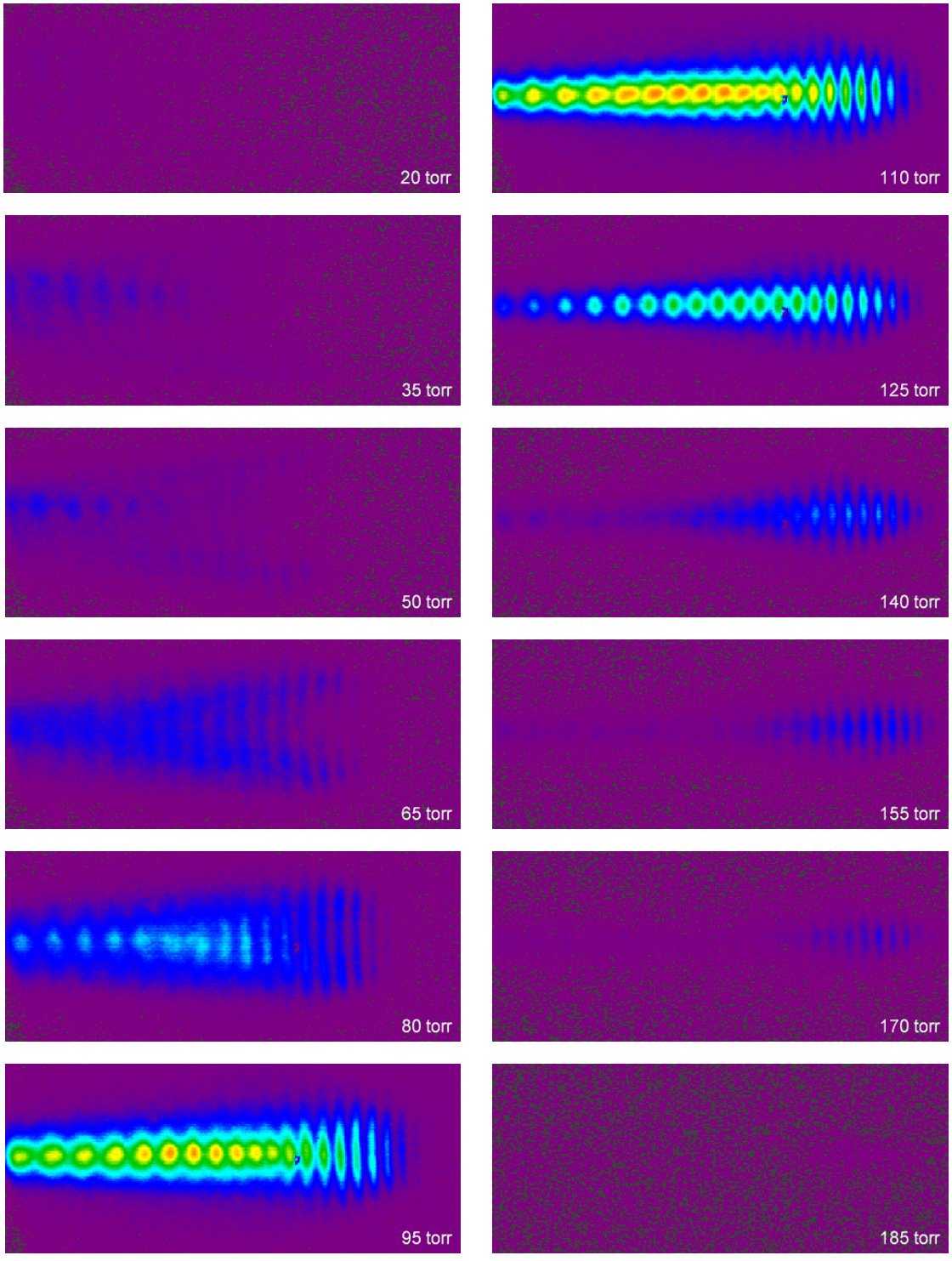

Fig. 3.8 Harmonic signal for several different pressures in helium.

3.5 Probing with Counter-Propagating Light

Fig. 3.9 is a graph of the intensity of selected harmonics as a function of pulse collision point for harmonics generated in 55 torr of neon. The counter-propagating pulse is long enough to interact with the forward going pulse for a total of ~2 mm at a time, and the collision point was scanned over a total distance of ~12 mm. Zero represents the position of the foil, and negative numbers correspond to positions inside the cell. The harmonics are generated with optimal aperture and focus position. When the counter-propagating light collides with the forward pulse deep inside the cell, the harmonic signal is quite strong, but as the collision zone nears the exit of the cell, suppression is evident. The data suggests that the harmonics are generated in a fairly narrow region just inside

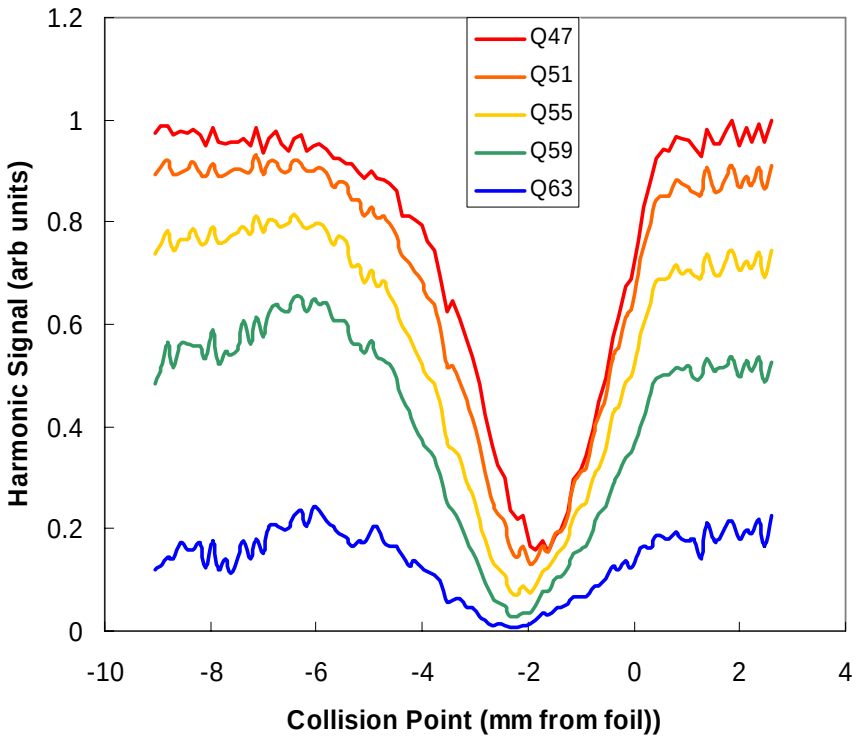

Fig 3.9 Intensity of selected harmonics (orders 47-63) as a fraction of maximum vs. counter-propagating pulse collision point for harmonics generated neon at 25 torr with optimal aperture and focal position.

the foil exit of the cell. Note that the suppression of the harmonics is nearly total and that it takes place over a 2-mm distance. A shorter counter-propagating pulse would not suppress the emission as completely.

Fig 3.10 shows a similar scan with the same counter-propagating pulse under conditions where the original signal is weak (neon at 30 torr with the laser focus moved 6 mm further in from the foil). Phase matching is poor for these conditions, but it is improved by suppressing harmonic production in regions with opposing phase as suggested in Ref [19]. The graph shows evidence of zones of alternating phase as the harmonic signal peaks and dips. Despite these improvements with quasi phase matching, we have not discovered a regime where enhancements exceed the best harmonics generated under optimal conditions. This suggests that the harmonics are already well phase matched when generating conditions are optimized.

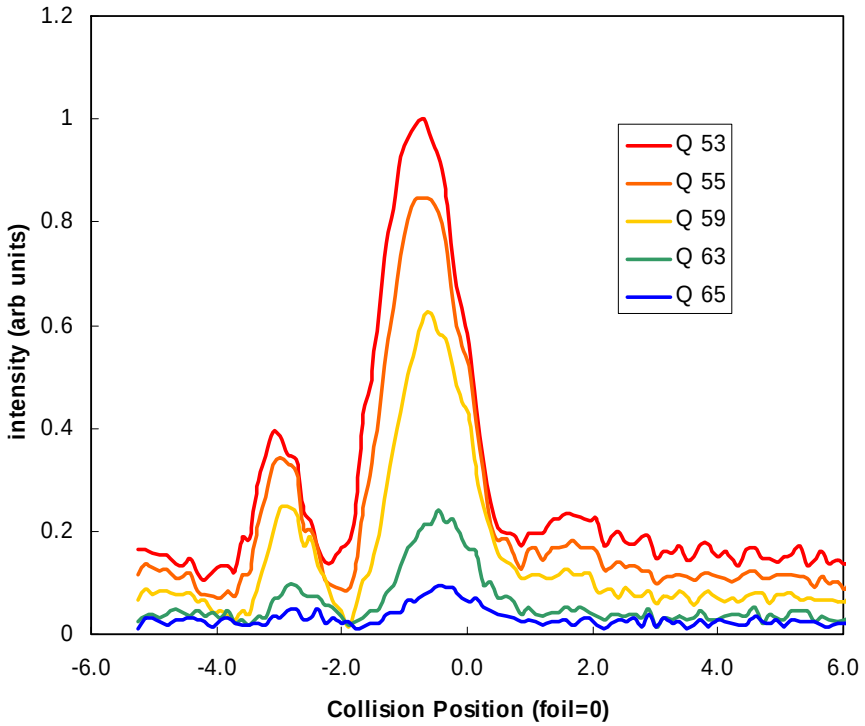

Fig. 3.10 Intensity of selected harmonics as a fraction of maximum vs. counter-propagating pulse collision point for neon at 30 torr and the focus 6mm upstream from optimal.

Using counter-propagating light to probe the harmonic signal generated in helium yields quite different results. Fig. 3.11 shows a counter-propagating scan in helium under optimal conditions. We were unable to significantly suppress the harmonic signal with counter-propagating light, even though it interacted with the forward pulse over a ~2 mm distance as before. This suggests that the harmonics in helium are generated (and phase matched) over a greater distance than in neon.

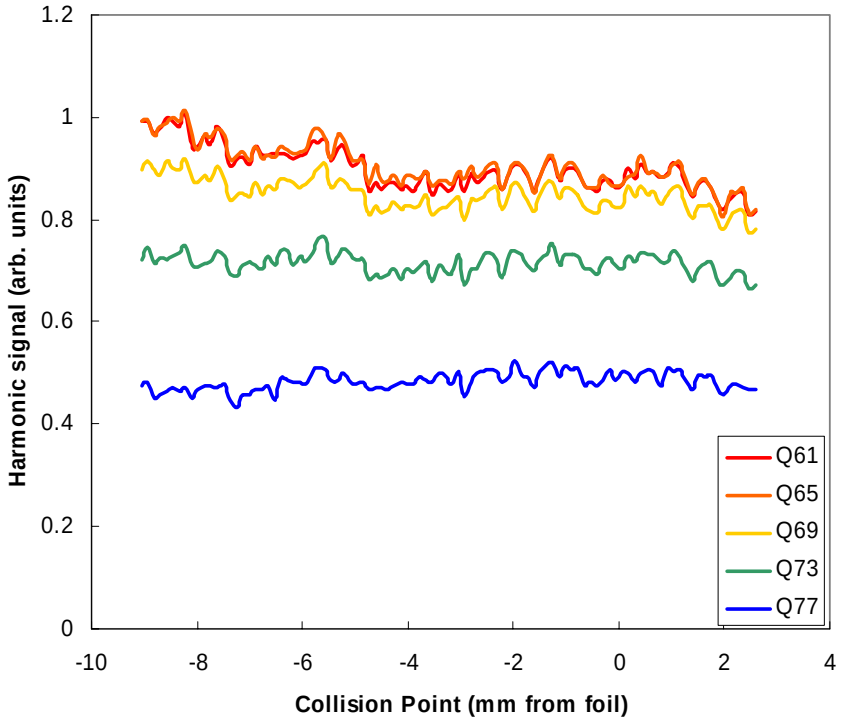

Fig. 3.11 Graph of harmonic signal as a fraction of individual maximum vs. counter-propagating pulse collision point for helium. No suppression is evident.

Differences in harmonic absorption by the two gases explain in part the differences in the harmonic generation depths as characterized by the counter-propagating light. Because the harmonics are phase matched over such a long distance, re-absorption becomes an important limiting factor. This is confirmed and discussed further in section 3.6. Transmission of the 71st harmonic through 2 mm of 55 torr neon is

29%. The 71st harmonic can propagate in helium at 110 torr for a distance five times longer with the same level of absorption [25].

3.6 Absorption Measurements Using a Secondary Cell

Fig 3.12 compares the theoretical transmission of high harmonics through both helium and neon with our measurements using the secondary cell described in section 2.5. Each graph shows the transmission versus the pressure for harmonics traveling through a fixed length (78 mm) of the same gas species that produced the harmonics. Again, no harmonics are generated in the secondary cell because the laser intensity there is much lower. The theoretical data was obtained from the website of The Center for X-ray Optics at Lawrence Berkeley National Laboratory [25]. The accuracy of the

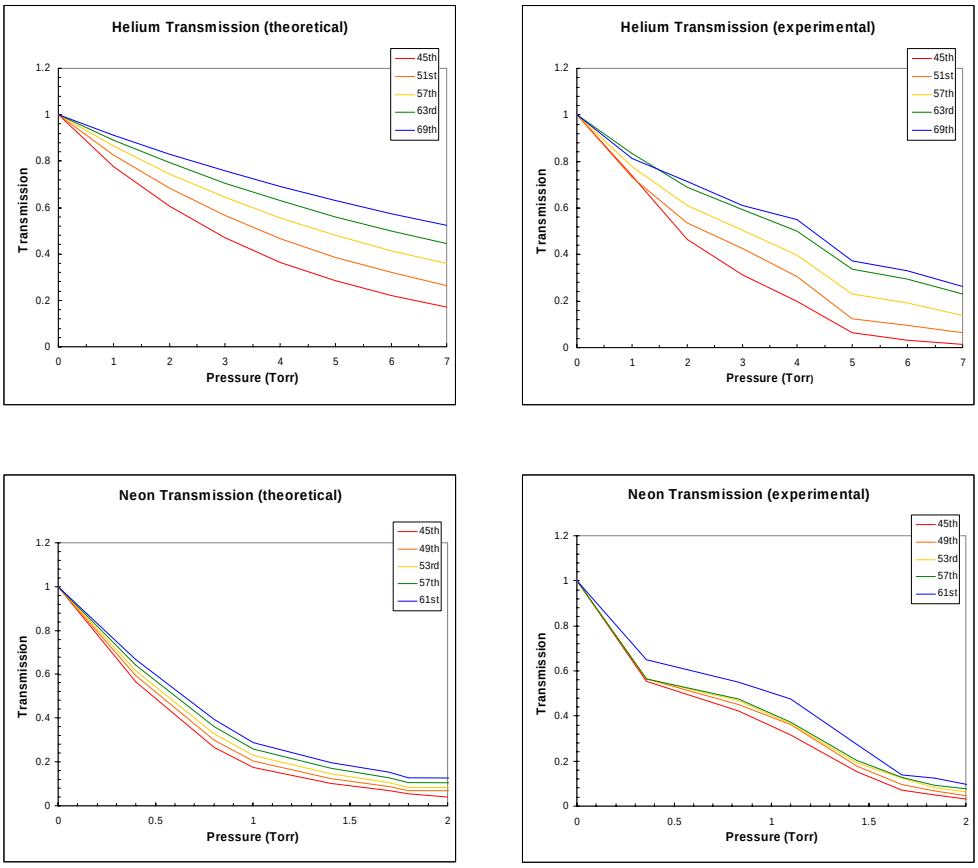

Fig. 3.12 Transmission vs. pressure for helium and neon.

experimental data is somewhat limited due to the sensitivity of the gauge, which reads to the nearest whole torr. Measurements in neon relied in part on a Varian Sentorr gauge that can read pressure in finer increments but has an unknown calibration for helium. Though there are differences between the experimental and theoretical data, the general trends of the two agree. Fig 3.13 shows images of the harmonics from which the experimental graph data was acquired. Each frame shows the harmonic signal as the pressure in the secondary cell is varied. The numerical data makes it possible to find the product of pressure and length for which a particular harmonic's transmission falls below 9%, which is the criterion for reaching the re-absorption limit mentioned in section 1.2. For example, the 45^{th} harmonic in neon drops to 9% transmission at around 1.5 torr in the 78 mm cell, suggesting the pressure-length product at which the re-absorption limit is reached is about 120 mm-torr. Since our harmonics are generated at an optimal pressure of 55 torr in neon, the necessary length to reach the re-absorption limit is only about 2 mm. In helium, the necessary pressure-length product to reach the re-absorption limit is over 900 mm-torr for the 51^{st} harmonic, and is even greater for higher harmonic orders, which means that harmonics generated at the optimal pressure of 110 torr must be phase matched over almost 10 mm to reach the re-absorption limit.

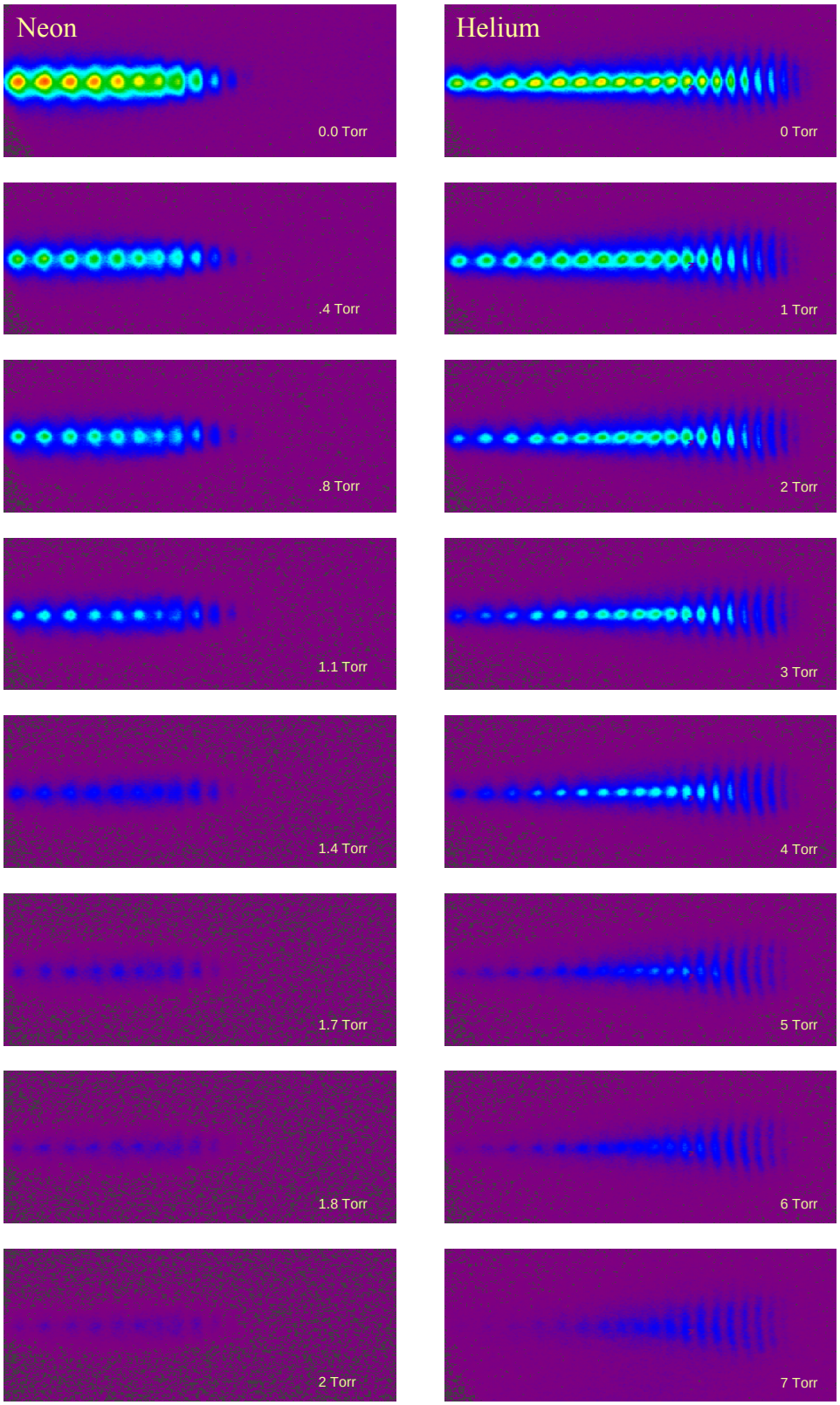

Fig. 3.13 Harmonic output for several pressures of absorbing gas in helium and neon.

Chapter 4: Summary and Conclusions

We have studied harmonic orders in the range 50-100 generated in a semi-infinite gas cell filled with neon or helium. We observed harmonic generation as a function of focal position relative to the cell exit foil, gas pressure, and diameter of an aperture at the focusing lens. Using counter-propagating light to probe harmonic generation allowed us to document the presence or absence of phase zones in an intense laser focus for different harmonic generating conditions. Direct measurements of re-absorption confirmed our understanding of its role in the HHG process.

Harmonic generation in the two gases shows similar behavior, the most pronounced difference being that helium produces more orders, up to the low 90s. Neon only produces orders through the 70s. A semi-infinite cell produces brighter harmonics in both gases than cells shorter than a centimeter. The optimal focal position (under vacuum conditions) for helium was 8 mm further back from the foil than it was for neon. Optimal pressure for harmonic production in the two gases differed. Though there was some dependence on focus position, a typical optimal pressure in neon was 55 torr, while the optimal pressure for helium was ~110 torr. Harmonics exhibit significant enhancement when the beam is restricted with an aperture at the focusing lens. The optimal aperture diameter for both helium and neon was found to be about 8 mm**.** Counter-propagating light revealed that in neon, the harmonics are produced in a 2 mm region near the exit foil, while in helium, the harmonics are produced over a much longer distance. Consideration of absorption helps to explain these findings. Direct absorption measurements in a secondary cell show the re-absorption limit is reached for mid-range harmonics generated in 2 mm of neon at 55 torr. However, in helium at 110 torr,

harmonics would have to be generated and phase matched over 10 mm to reach the re-absorption limit, so some improvement to harmonic generation in helium may still be possible.

Probing our harmonic emission with counter-propagating pulses shows that phase-matching under optimized conditions occurs over distances much longer than expected. Optimizing aperture, focal position and pressure produces a single phase zone at least several millimeters long. Phase zones were also probed under less optimal conditions where it was possible to enhance harmonic production through quasi phase matching. However, the enhancements did not result in better harmonics than cases where the aperture, focal position and pressure were optimized. The measurements show that the phase-matching occurs over a much greater distance than anticipated when diffraction of the fundamental beam in a vacuum is considered. Whether the harmonics are actually phase matched over the entire distance, or if emission at different depths is generated at different radii could not be determined. The scans of harmonics as a function of focal position relative to the exit foil and of aperture radius show variations in the angular spread of the harmonics in the far field. These variations may offer clues to the interactions between the laser beam and the generating medium and may lead to better understanding of the how phase matching occurs. In any case, the observations are consistent with those reported by Takahashi et al. who interpreted bright harmonic emission as evidence of laser filimentaion within the gas medium [26].

Future research in our group will seek to show how and why this unexpected phase matching occurs. The research will persue the suggestion that laser beam filamentation is responsible [26]. The relationship between phase matching and

filamentation will be investigated using our unique counter-propagating light probe. Our group will also measure the absolute energy of the harmonics under our generating conditions to determine conversion efficiency, which will allow our results to be directly compared with the results of other researchers in the field.

References

1. Opto & Laser Europe, "EUV sources shape up for competition," IOP Publishing Oct. (2003), http://optics.org/articles/ole/8/10/3/1.
2. S. L. Voronov, "Controlling Laser High-Order Harmonic Generation Using Weak Counter-Propagating Light," *PhD Dissertation*, Brigham Young University (2003).
3. S. Kazamias, D. Douillet, F. Weihe, C. Valentin, A. Rousse, S. Sebban, G. Grillon, F. Auge, D. Hulin, and Ph. Balcou, "Global optimization of high harmonic generation," Phys. Rev. Lett. **90**, 193901 (2003).
4. R. Bartels, S. Backus, E. Zeek, L. Misoguti, G. Vdovin, I. P. Christov, M. M. Murnane, and H. C. Kapteyn, "Shaped-pulsed optimization of coherent emission of high-harmonic soft x-rays," Lett. to Nature **406**, 164 (2000).
5. E. Takahashi, Y. Nabekawa, and K. Midorikawa, "Generation of 10-μJ Coherent Extreme-Ultraviolet Light by use of High-Order Harmonics," Opt. Lett. **27**, 1920 (2002).
6. L. G. Gouy, "Sur une propriete nouvelle des ondes lumineuses," Compt. Rendue Acad. Sci. Paris, **110**, 1251 (1890).
7. P. Milonni and J. Eberly, *Lasers*, Wiley-Interscience (1989).
8. E. Constant, D. Garzella, P. Breger, E. Mevel, C. Dorrer, C. L. Blanc, F. Salin, and P. Agostini, "Optimizing high harmonic generation in absorbing gases: model and experiment," Phys. Rev. Lett. **82**, 1668 (1999).

9. E. Christensen “Direct Measurement Of Absorption Rates For Laser High-Order Harmonics Generated In Helium And Neon,” *Senior Thesis*, Brigham Young University (2005).

10. A. L’Hullier and P. Balcou, “High-Order Harmonic Generation in Rare Gases with a 1-ps 1053-nm Laser,” Phys. Rev. Lett. **70,** 774 (1993).

11. J.-F. Hergott, M. Kovacev, H. Merdji, C. Hubert, Y. Mairesse, E. Jean, P. Breger, P. Agostini, B. Carre, and P. Salieres, “Extreme-ultraviolet high-order harmonic pulses in the microjoule range,” Phys. Rev. A **66**, 021801(R) (2002).

12. E. A. Gibson, A. Paul, N. Wagner, R. a. Tobey, D. Gaudiosi, S. Backus, I. P. Christov, A. Aquila, E. M. Gullikson, D. T. Atwood, M. M. Murnane, and H. C. Kapteyn, “Coherent Soft X-Ray Generation in the Water Window with Quasi-Phase Matching,” Science **302**, 95 (2003).

13. E. A. Gibson, A. Paul, N. Wagner, R. a. Tobey, S. Backus, I. P. Christov, M. M. Murnane, and H. C. Kapteyn, “High-Order Harmonic Generation up to 250eV from Highly Ionized Argon,” Phys. Rev. Lett. **92**, 033001 (2004).

14. A. Rundquist, C. G. D. III, Z. Chang, C. Herne, S. Backus, M. M. Murnane, and H. C. Kapteyn, “Phase- Matched Generation of Coherent Soft X-Rays,” Science **280**, 1412 (1998).

15. Y. Tamaki, J. Itatani, Y. Nagata, M. Obara, and K. Midorikawa, “Highly efficient, phase-matched high-harmonic generation by a self-guided laser beam,” Phys. Rev. Lett. **82**, 1422 (1999).

16. E. Takahashi, Y. Nabekawa, T. Otsuka, M. Obara, and K. Midorikawa, "Generation of highly coherent submicrojoule soft x-rays by high-order harmonics," Phys. Rev. A **66**, 021802(R) (2002).

17. E. Takahashi, Y. Nabekawa, and K. Midorikawa, "Low-divergence coherent soft x-ray source at 13nm by high-order harmonics," Appl. Phys. Lett. **84**, 4 (2004).

18. A. Paul, R. A. Bartels, R. Tobey, H. Green, S. Weiman, I. P. Christov, M. M. Murnane, H. C. Kapteyn, and S. Backus, "Quasi-phase-matched generation of coherent extreme-ultraviolet light," Lett. to Nature **421**, 51 (2003).

19. J. B. Peatross, S. Voronov, and I. Prokopovich, "Selective zoning of high harmonic emission using counter-propagating light," Opt. Express **1,** 114 (1997).

20. S. L. Voronov, I. Kohl, J. B. Madsen, J. Simmons, N. Terry, J. Titensor, Q. Wang, and J. Peatross, "Control of Laser High Harmonic Generation with Counter-Propagating Light," Phys. Rev. Lett. **87**, 133902 (2001).

21. J. Peatross, J. R. Miller, K. R. Smith, S. E. Rhynard, and B.W. Pratt, " Phase matching of high-order harmonic generation in helium- and neon-filled gas cells," J. Mod Opt **51**, 2675 (2004).

22. J. R. Sutherland, E. I. Christensen, N. D. Powers, S. E. Rhynard, J. C. Painter, and J. Peatross, "High harmonic generation in a semi-infinite gas cell," Opt. Express **12,** 4430 (2004).
http://www.opticsexpress.org/abstract.cfm?URI=OPEX-12-19-4430.

23. S. Kazamias, F. Weihe, D. Douillet, C. Valentin, T. Planchon, S. Sebban, G. Grillon, F. Auge, D. Hulin, and P. Balcou, "High order harmonic generation optimization with an apertured laser beam," Eur. Phys. J. D **21**, 353 (2002).

24. K. Smith, “Phase Matching of Laser High Harmonic Generation in a Semi-infinite Gas Cell,” Honors Thesis, Brigham Young University (2004).

25. Center for X-Ray Optics, “Gas Filter Transmission,” http://www.cxro.lbl.gov/optical_constants/gastrn2.html

26. V. Tosa, E Takahashi, Y. Nabekawa and K. Midorikawa, “Generation of high-order harmonics in a self-guided beam,” Phys. Rev. A. **67**, 063817 (2003).